ACS APPLIED MATERIALS & INTERFACES

Research Article

www.acsami.org

Quasi-Immiscible Spreading of Aqueous Surfactant Solutions on Entangled Aqueous Polymer Solution Subphases

Ramankur Sharma,[†,‡] Timothy E. Corcoran,[#] Stephen Garoff,[*,‡,§] Todd M. Przybycien,[†,‡,∥] Ellen R. Swanson,[‡,⊥,○] and Robert D. Tilton[†,‡,∥]

[†]Department of Chemical Engineering, [‡]Center for Complex Fluids Engineering, [§]Physics Department, [∥]Department of Biomedical Engineering, [⊥]Department of Mathematical Sciences, Carnegie Mellon University, Pittsburgh, Pennsylvania 15213, United States

[#]Department of Medicine, University of Pittsburgh, Pittsburgh, Pennsylvania 15260, United States

[○]Department of Mathematics, Centre College, Danville, Kentucky 40422, United States

Supporting Information

ABSTRACT: Motivated by the possibility of enhancing aerosol drug delivery to mucus-obstructed lungs, the spreading of a drop of aqueous surfactant solution on a physically entangled aqueous poly(acrylamide) solution subphase that mimics lung airway surface liquid was investigated. Sodium dodecyl sulfate was used as the surfactant. To visualize spreading of the drop and mimic the inclusion of a drug substance, fluorescein, a hydrophilic and non-surface-active dye, was added to the surfactant solution. The spreading progresses through a series of events. Marangoni stresses initiate the convective spreading of the drop. Simultaneously, surfactant escapes across the drop's contact line within a second of deposition and causes a change in subphase surface tension outside the drop on the order of 1 mN/m. Convective spreading of the drop ends within 2−3 s of drop deposition, when a new interfacial tension balance is achieved. Surfactant escape depletes the drop of surfactant, and the residual drop takes the form of a static lens of nonzero contact angle. On longer time scales, the surfactant dissolves into the subphase. The lens formed by the water in the deposited drop persists for as long as 3 min after the convective spreading process ends due to the long diffusional time scales associated with the underlying entangled polymer solution. The persistence of the lens suggests that the drop phase behaves as if it were immiscible with the subphase during this time period. Whereas surfactant escapes the spreading drop and advances on the subphase/vapor interface, hydrophilic dye molecules in the drop do not escape but remain with the drop throughout the convective spreading. The quasi-immiscible nature of the spreading event suggests that the chemical properties of the surfactant and subphase are much less important than their physical properties, consistent with prior qualitative studies of spreading of different types of surfactants on entangled polymer subphases: the selection of surfactant for pulmonary delivery applications may be limited only by physical and toxicological considerations. Further, the escape of surfactant from individual drops may provide an additional spreading mechanism in the lung, as hydrodynamic and/or surface pressure repulsions may drive individual droplets apart after deposition.

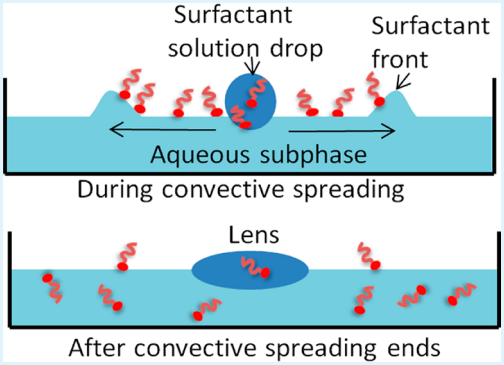

KEYWORDS: *Marangoni flow, surfactant spreading, surfactant transport, pulmonary drug delivery*

1. INTRODUCTION

A significant problem often encountered when administering aerosolized medications in the treatment of chronic obstructive pulmonary diseases is that the drug does not effectively access all the portions of the lungs,[1−3] thereby decreasing efficacy. An important example is the nonuniform deposition of inhaled aerosols in the treatment of bacterial infections of the lungs of cystic fibrosis patients, due to obstructions associated with inflammation and mucus plaques.[4−6] Current inhalation therapies rely on aerodynamic mechanisms to disperse and distribute drug inside lungs after inhalation.[6] A recently proposed strategy to improve drug penetration downstream of lung obstructions is to add surfactant to the aerosol to harness surface tension gradient driven Marangoni flows which can carry drugs along the airway surface liquid (ASL) after aerosol droplet deposition.[6,7] The use of surfactants in the lungs is a relatively long-standing practice in the context of bolus surfactant replacement therapy for neonatal acute respiratory syndrome.[8−10] In vitro proof of surfactant-enhanced spreading on complex aqueous subphases that mimic the ASL[6,7] and evidence for altered lung clearance patterns after aerosolized surfactant inhalation in humans has been reported.[5]

Marangoni spreading driven by soluble and insoluble surfactants on liquid subphases has been studied. In some cases, the source of the surfactant is a confined surfactant film which is then released, causing the spreading,[11,12] a neat

Received: February 28, 2013
Accepted: May 24, 2013
Published: May 24, 2013

   dx.doi.org/10.1021/am400762q | ACS Appl. Mater. Interfaces 2013, 5, 5542−5549

surfactant drop,[13−19] or a surfactant solution drop.[20−25] Several recent reviews detail the existing work on surfactant assisted spreading on liquid subphases.[26−29] Since a surfactant-containing drop has a lower surface tension than the underlying subphase, as it touches the subphase, the capillary imbalance at the three-phase contact line creates the stress that drives the drop to spread. Surface tension gradients develop across the drop/vapor interface and drop/subphase interface and across the subphase surface (i.e., the subphase/vapor interface). The surfactant escapes from the deposited drop's contact line and moves across the subphase/vapor interface ahead of the drop. The surface Marangoni stress also drives a flow in the subphase, and at the leading edge of the spreading surfactant concentration profile, a capillary ridge forms and moves across the subphase.[26,29] The Marangoni or convective spreading of the drop ceases as the three interfacial tensions, drop/vapor, drop/subphase, and subphase/vapor, evolve and the capillary balance is established. Although the dynamics of the drop and surfactant front are fairly well understood at this time, a clear picture of the postspreading fate of each component of the surfactant solution drop on complex liquid subphases is lacking. Knowledge of the latter is the key to designing optimum surfactant formulations.

In this work, we study spreading in a system mimicking key characteristics of pulmonary drug delivery, and determine the postspreading fate of formulation components comprising surfactant, water, and a hydrophilic non-surface-active solute that serves as a model drug compound. We have focused on the spreading of individual microliter drops of mock drug formulations rather than aerosols to facilitate experimental interrogation of the system. While we expect that the quantitative aspects of the postdeposition spreading of individual drops will depend on the extent of the system, including both drop size and surfactant inventory, the underlying mechanism determining the qualitative behavior should be independent of drop size. Here, microliter drops of aqueous sodium dodecyl sulfate solutions are deposited on physically entangled aqueous poly(acrylamide) (PA) solution subphases. The entangled polymer solution mimics pulmonary mucus, a 95 wt %/wt aqueous, viscoelastic solution of mucin glycoprotein, DNA, and various other solutes present in different amounts depending on the health of the lungs.[30] The principal component of airway mucus is an entangled, randomly coiled network of mucin glycoproteins[31] with molecular weights ranging from about 1 to 10 MDa.[32] Mucus is heterogeneous and optically opaque at relevant concentrations. To avoid experimental, compositional, and chemical complexities in this study, physically entangled aqueous solutions of high molecular weight PA were used as the liquid subphase. The 5−6 MDa PA used is similar to the molecular weight of porcine gastric mucin which we have used in prior qualitative spreading studies.[6,7] The choice of soluble surfactant, sodium dodecyl sulfate, was made for convenience, as our prior work demonstrated that spreading behavior was qualitatively similar for aqueous solutions of anionic, cationic, and nonionic surfactant deposited on both PA and porcine gastric mucin subphases.[7]

We see a cascade of events and time scales. Upon drop deposition, surfactant crosses the contact line and rapidly moves across the surface ahead of the contact line at speeds on the order of cm/s. Drop spreading ceases after a few seconds, but surfactant that has spread on the subphase outside the drop dissolves into the subphase over time scales of tens of seconds. Despite the drop content's complete miscibility with the aqueous subphase, the drop remains as a "lens" (a drop with nonzero contact angle) on the surface for several minutes after both spreading and surfactant dissolution have completed; during this period, the drop and subphase behave as if they were immiscible. The hydrophilic dye stays with the drop rather than convecting across the subphase surface with the surfactant.

2. MATERIALS AND METHODS

2.1. Materials. Subphases were either a 1 wt %/wt aqueous solution of poly(acrylamide) (density 1.0 g/mL) or a 75% v/v glycerol solution in water (density 1.2 g/mL). The poly(acrylamide) (PA; molecular mass 5 000 000−6 000 000 g/mol, CAS# 9003-05-8) was purchased from Polysciences (Cat# 02806). The glycerol (≥99.5%, CAS# 56-81-5) was used as received from Sigma Aldrich (Cat# G7893) and was maintained in a sealed bottle until use. The surfactant was anionic sodium dodecyl sulfate (SDS; Electrophoresis grade, CAS# 151-21-3), purchased from Fisher Scientific (Cat# BP166-100) and used as received. The subphases were buffered to pH 9 using prepackaged buffer salts (Hydrion Buffer Chemvelope pH 9.00) from Micro Essential Laboratory (Cat# 280-9.00); these contain 20−30 wt %/wt sodium carbonate (CAS# 497-19-8) and 70−80 wt %/wt sodium bicarbonate (CAS# 144-55-8). Fluorescein dye (laser grade 99%, CAS# 2321-07-5) was purchased from Fisher Scientific (Cat# AC41062-0010) and used as received. All the glassware used for experiments was cleaned sequentially using ethanol, acetone, and deionized water several times and then dried under a nitrogen stream. The deionized water was obtained from a Milli-Q Academic unit (Millipore Corporation) and had a resistivity of 18 MΩ·cm, pH ∼ 6, a surface tension of 72.7 ± 0.7 mN/m (where the quoted uncertainty here and elsewhere in this article is the standard error of the mean), and a total organic content <10 ppb. Pyrex glass Petri dishes of radius 4.5 or 7.5 cm were used to contain the liquid subphase. All the experiments were conducted at room temperature (23 ± 1 °C).

Both the subphase and surfactant solutions were buffered to pH 9 to maximize the quantum yield of the fluorescein dye. The 1 wt %/wt entangled PA solutions were prepared by adding PA powder in increments of 2 g per day to 750 mL of water in a 1000 mL bottle under nitrogen with continuous gentle mixing on a gyrotory water bath shaker (New Brunswick Scientific, model G79, speed "4") for 20−25 days to ensure solution homogeneity. The last 2−3 g were added in an increment of 1 g per day, since it took more time to mix the solution as it became more viscous. After the final addition of PA powder, 250 mL of water was added along with the buffer salts to the PA solution, and stirring continued for 2−3 more days until the solution had become homogeneous. The entanglement concentration of this PA in solution was determined to be approximately 0.45 wt %/wt by measuring the viscosity of PA solutions as a function of concentration with an Ubelhode capillary viscometer (see the Supporting Information).

The surfactant solutions contained 10^{-4} M fluorescein dye to visualize the spreading of drops. Stock solutions containing dye were covered with aluminum foil to minimize photobleaching. The addition of fluorescein dye and buffer salts to the Milli-Q water did not change the surface tension, measured as $\gamma = 72.2 \pm 0.7$ mN/m. SDS solutions were used within 6 days of preparation to minimize the formation and influence of dodecanol and sulfate hydrolysis products.

2.2. Surface Tension. All liquid/vapor surface tensions were measured with a Wilhelmy pin apparatus as described elsewhere.[33] The surface tension of the 1 wt %/wt aqueous PA solution was measured immediately after pouring into the Petri dish and was found to be 71.2 ± 0.3 mN/m (n = 15 trials), consistent with surface tension values reported elsewhere.[34,35] A decrease in PA solution surface tension with time was recorded (see Figure 1). This is likely due to the slow adsorption of polymer chain segments to the PA solution/vapor interface and/or a localized increase in polymer concentration at the interface due to solvent evaporation as reported for other polymer solutions.[36]

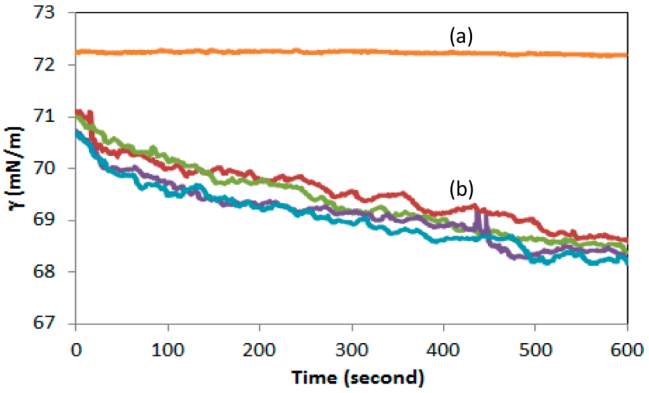

Figure 1. Reduction of PA/vapor interfacial tension with time. (a) A representative flat baseline observed for water at 72.2 mN/m. (b) Several typical sets of data showing the decrease of PA/vapor interfacial tension with time.

The surface tension of the subphase was measured by the Wilhelmy pin technique as a function of time before and after drop deposition in a region well outside the final area covered by the drop (Figure 2).

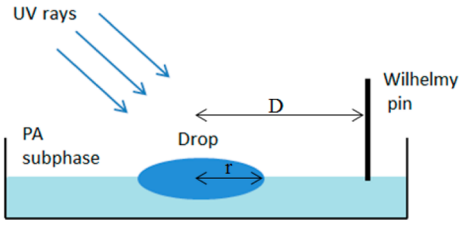

Figure 2. Surface tension monitoring technique with simultaneous visualization of the spreading drop and measurement of the local surface tension external to the drop. $D \sim 4$ cm, where D is the distance between the pin and the deposited drop, and $r \sim 2$ cm, where r is the typical radius of a drop after convective spreading ends.

The depth of the subphase in all spreading experiments was at least 0.5 cm. The likelihood of the subphase rupture during drop spreading was assessed via computation of a gravitational parameter[17]

$$G = \rho g H^2/(\gamma_0 - \gamma_m) \approx 200 \quad (1)$$

giving the ratio of gravity to Marangoni forces, where ρ is the subphase density ($\sim$1000 kg/m^3), g is acceleration due to gravity ($\sim$10 m/s^2), H is the subphase thickness ($\sim$0.5 cm), and $(\gamma_0 - \gamma_m)$ is the difference between the surface tension of clean subphase and surfactant covered subphase ($\sim$1 mN/m as discussed in section 3.2). Theoretical models indicate that large values of $G \gg 1$ preclude subphase rupture during spreading.[17] The pin was positioned 2 cm away from the walls of the dish. For the surfactant concentrations and deposited drop volumes used here, these Petri dishes were sufficiently large that the spreading drops never reached the dish edge or the Wilhelmy pin. The PA solution subphase was left to gravitationally level itself for 5 min after pouring into a Petri dish. The rate of change of the PA solution surface tension slowed significantly after 5 min, but the slow decrease never fully stopped on the time scale of the experiments. Before drop deposition, the pin was lowered to the PA subphase and surface tension reading was zeroed to record the change in subphase surface tension, or the surface pressure, caused by any surfactant escaping the drop after deposition.[19,33]

A single surfactant solution drop was deposited 5 min after pouring PA into a Petri dish, and the phenomena investigated here occurred between 5 and 7 min after pouring. At longer times, a "skin" could be observed to form on the PA subphase due to evaporation. Evaporation enriches the PA/vapor interface in polymer and is observed to alter the rheological properties of the interface.[37−39] Skinning was observed by scratching the PA solution surface with a clean pipet and monitoring the shadowgram formed under coherent laser illumination. Scratches made within 10 min after pouring the PA solution disappeared quickly, but scratches made on solutions more than 10 min after pouring were persistent, suggesting the formation of the skin.

Eppendorf Research Plus micropipets (0.1 to 10 and 1 to 10 μL by volume) were used for dispensing surfactant solution drops. Before dispensing the drop, the outside of the tip was wiped with a Kimwipe to remove any excess solution that would otherwise be carried into the subphase. This precaution was necessary to ensure reproducible extents of spreading. Low volume drops (1 μL) were placed on the subphase with a minimum of kinetic energy by gently touching the drop formed at the end of the micropipet tip to the subphase surface. Drops were deposited 4 or 6 cm away from the pin, and a hand-held UV lamp (Mineralight Lamp model UVGL-25, Multiband UV-254/366 nm, 115 V, 60 Hz, and 0.16 A) was used to detect the spreading of the fluorescent-dye-containing drop, as shown in Figure 2. Depositions were designed such that the spreading drops never touched the Wilhelmy pin, as typical spread drop radii were $\sim$2 cm and never exceeded $\sim$2.5 cm, based on visual observation.

2.3. Imaging the Solution Lens on the Subphase. To determine whether or not the final state of the spread solution drop was a lens of finite thickness, a Ronchi ruling-based technique was used[40] (see Figure 3a). A liquid lens distorts the image of the ruling as light rays are refracted at the curved lens/vapor interface. Spreading experiments were repeated in glass Petri dishes placed on top of a Ronchi ruling (2 in × 2 in/150 lines), and the ruling was imaged through the fluid with a microscope (Nikon AZ100) equipped with a AZ-Plan Apo 0.5× objective (NA: 0.05/WD: 54 mm) using illumination from below. The images obtained from the Ronchi ruling technique were processed using Image J (National Institutes of Health) software to see the lens more clearly. Processing consisted of background subtraction, contrast enhancement by 30%, followed by the "smooth" operation, and finally the "find edges" operation. Transient surface tension measurements and Ronchi ruling observations were performed in separate experiments, as these two techniques cannot be performed simultaneously with our experimental setup.

Fluorescence microscopy was used to detect the fate of the dye after drop deposition. Instead of using the Ronchi ruling with trans-illumination, UV excitation was used with epi-illumination on the same microscope to detect the fluorescent dye. The microscope could be switched between the two imaging modes during the same spreading experiment so that fluorescence and Ronchi ruling images were recorded on the same lens with only an approximate 20 s time delay between images. The Ronchi ruling image shows the extent of the lens, while the fluorescence image shows the location of the dye. Comparison therefore reveals whether or not dye escapes the lens.

3. RESULTS AND DISCUSSION

3.1. Fate of the Solvent in the Drop. Figure 3a shows direct evidence that the aqueous SDS solution drop remains on the surface of the aqueous PA solution subphase for long times after the spreading of the drop has ceased despite their complete miscibility. The distorted image shows this lens has finite thickness and nonzero contact angle. While the particular image in Figure 3a is taken 3 min after deposition, distortions of the Ronchi ruling images indicate that a lens of solution can remain for several minutes after drop deposition. All other dynamic processes, including the drop spreading, movement of the surfactant over the subphase, and surfactant dissolution into the subphase, are completed within a few to tens of seconds (discussed below in section 3.2). We have verified that there is no phase separation when SDS is added to a PA solution, so this temporary apparent immiscibility is not due to a separate phase forming at the lens/subphase interface. As a control, we observe that a drop of PA solution deposited on the PA subphase disappears in a few seconds. We also see persistence

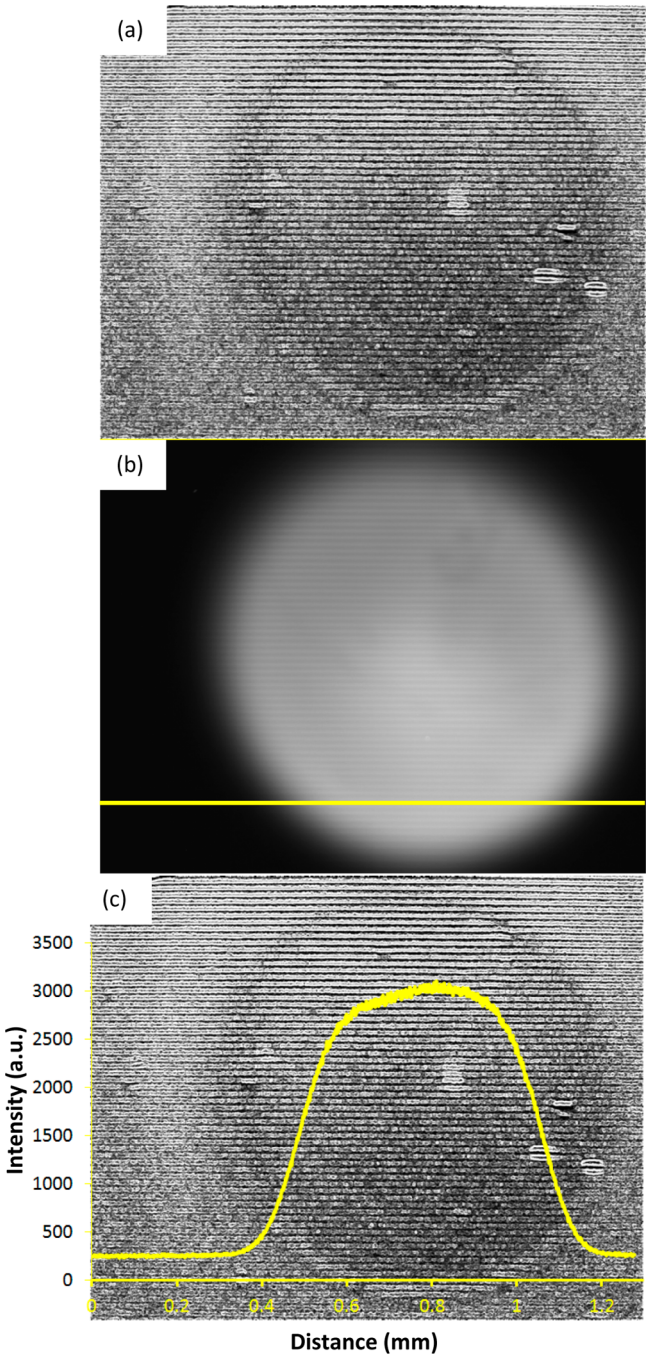

Figure 3. (a) Ronchi ruling image showing a lens formed when 0.3 μL of 1 mM SDS solution drop is deposited on a 1 wt %/wt PA subphase. (b) Fluorescein dye viewed in epi-illumination mode. The horizontal yellow line shows the line scan of intensity plotted in part c where the intensity profile is superimposed on the Ronchi ruling image at the same position of the line scan. Images a and b were captured ~3 min after drop deposition. The time difference between images a and b is ~20 s.

of aqueous drops, with or without surfactant, after deposition on a simple molecular subphase of glycerol–water (75% v/v). This demonstrates that this behavior is not specific to the poly(acrylamide) subphase. Lenses of pure aqueous drops persist for a shorter time (lasting for ~5 min) on glycerol–water subphases than the lenses formed on the PA solution subphases (~10 min).

These observations show that the fluid flow during drop spreading does not cause convective intermixing of the drop and subphase contents. After spreading, diffusion must be responsible for contents mixing and the eventual disappearance of the lens/subphase interface. During this process, a capillary balance determines the shape of the lens. The aqueous lens/aqueous subphase interfacial tension must be extremely low, so that the lens/vapor and subphase/vapor interfacial tensions establish the capillary balance. Even in the case of the simple molecular subphase (glycerol–water (75% v/v)), diffusion is sufficiently slow that the lens remains for several minutes after spreading has ceased. The much longer times observed for the entangled polymer subphase likely arise because the movement of the polymer chains into the lens is slowed due to requirement of the polymer chains to disentangle from the network and penetrate the lens. We have observed (data not shown) that at the same mass concentration, 1 wt %/wt, the persistence times of the lenses on the subphase are shorter for 1 MDa PA, which we interpret as due to the decreased entanglement of the smaller polymer chains.

3.2. Fate of the Surfactant. Experiments were performed with 1 μL drops of aqueous fluorescein solutions containing either no surfactant as a negative control or SDS surfactant deposited on a 1 wt %/wt PA solution subphase in a 4.5 cm (radius) Petri dish. The typical SDS concentration used in the drop phase was 2 mM, above the critical micelle concentration (CMC). The CMC of the pH 9 buffered SDS solution containing 10^{-4} M fluorescein dye was determined to be approximately 1 mM from the break in the surface tension isotherm plotted in Figure 4. This is smaller than the 8.3 mM CMC of SDS in DI water but consistent with the CMC of SDS in solution with 100 mM NaCl.[41]

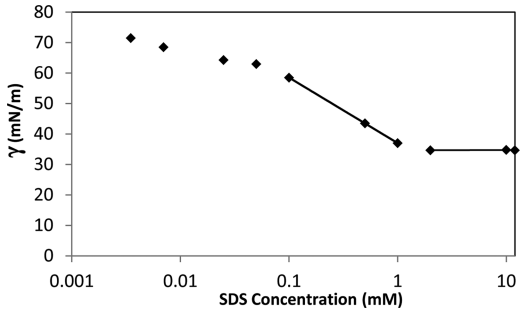

Figure 4. Surface tension of SDS solution in 10^{-4} M fluorescein dye and pH 9 buffer solution. The uncertainty in surface tension values is ±0.7 mN/m. The CMC is determined as ~1 mM from the intersection of the two least-squares regression lines.

When a 1 μL surfactant-free drop was deposited on a PA subphase 4 cm away from the Wilhelmy pin, no surface tension change was recorded that could be distinguished from the 0.2 mN/m noise level in the measurement. The absence of any detectable surface tension change in the control experiment indicates that not only was there no change in subphase surface composition remote from the deposited solution drop but also that no mechanical disturbance possibly caused by the drop deposition procedure is sufficient to perturb the force on the Wilhelmy pin in a way that would produce an apparent surface tension change.

In contrast, the 2 mM SDS solution drops caused a surface tension decrease of 1.4 ± 0.1 mN/m (n = 10) 4 cm away from the deposition point, and well outside the final spread area of

the drop (occurring at $t \sim 300$ s in Figure 5; $t = 0$ corresponds to the time when PA was poured into Petri dish). The onset of

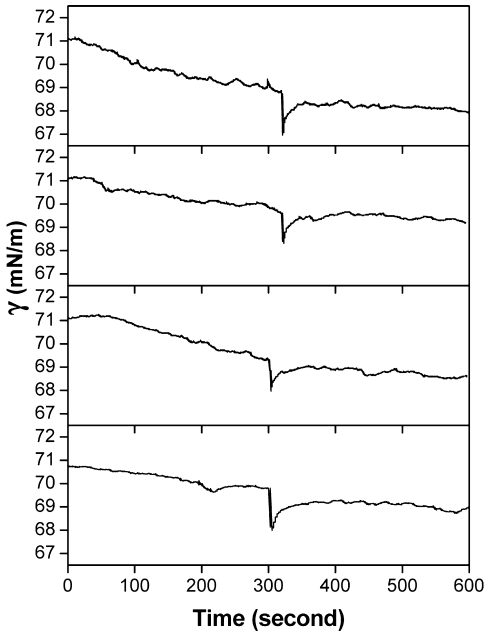

Figure 5. Representative plots showing the surface tension change before and after a 1 μL drop of 2 mM SDS is deposited on the PA solution subphase, 4 cm away from the Wilhelmy pin in a 4.5 cm radius dish. The drop was deposited at $t \sim 300$ s.

the decrease in surface tension occurs within 1 s of drop deposition. This was followed by a surface tension recovery as discussed below. The surface tension decrease demonstrates that surfactant crossed the contact line and convected across the subphase due to Marangoni stresses. Simultaneously, drop spreading was observed under a hand-held UV lamp. The spreading drop never touched the pin and eventually took the shape of a bright circular spot with a well-defined boundary.

The surfactant concentration in the drop controls the magnitude of the surface tension decrease. When a 1 μL drop containing only 1 mM SDS solution was deposited on the PA subphase, the trends were similar but the surface tension decrease was only 0.8 ± 0.1 mN/m (n = 10) (see the Supporting Information). This indicates that the surfactant inventory in the drop influences the maximum surfactant surface concentration that can be established on the subphase surface outside the deposited drop. Although the magnitude of the recorded surface tension dip is specific to this particular system and the extent of the subphase surface area, the phenomenon of surfactant escaping across drop contact line has been observed for different systems.[7,33]

As in our experiments with the Ronchi ruling images, visual observation under UV illumination consistently showed that the final extent of spreading was finite and that the final region covered by the lens of spread solution had a well-defined boundary. The convective spreading process of the drop was completed in a few seconds. This convective spreading is driven by the convective motion caused by Marangoni stresses and is much faster than the surface or bulk diffusion of SDS.

The dominance of Marangoni-driven convective flows in these systems is further supported by analysis of the relative rates of convective and diffusive transport, as represented by the Peclet number (Pe), and of the relative magnitudes of the imposed Marangoni stress and the viscous drag, as represented by a Maragoni number (M). The Peclet number, defined as

$$Pe \equiv \frac{LU}{\mathcal{D}} \sim o(10^6) \tag{2}$$

where L is a characteristic length scale along the spreading film, here ~1 cm, U is the observed convective velocity, here ~1 cm/s, and $\mathcal{D}$ is the surface or bulk diffusivity of SDS found for a water subphase, on the order of 10^{-10} m^2/s[42,43] is very large. This indicates that convective transport dominates diffusive transport. Defining a Marangoni number as

$$M \equiv \frac{(\gamma_o - \gamma_m)H}{\mu LU} \sim o(1) \tag{3}$$

where $(\gamma_o - \gamma_m)$ is the difference between the maximal and minimal value of subphase surface tension, ~1 mN/m as represented by the observed surface tension dip in Figure 5, H is the thickness of the subphase, ~0.5 cm, and μ is the viscosity of subphase, ~40 cP respectively, we find that the imposed Marangoni stress is on the same order of magnitude as the viscous drag opposing the convective flow. This suggests that Marangoni stresses are responsible for the observed flow.[28] Evaluation of an alternative Peclet number, as suggested by Matar et al.,[42] to express the relative magnitudes of the convective flow rate induced by Marangoni stresses and the diffusive transport rate and defined as

$$Pe_s \equiv \frac{SH}{\mu\mathcal{D}} \sim o(10^8) \tag{4}$$

where S is the spreading coefficient, here ~40 mN/m, also gives a large value indicative of the dominance of Marangoni stress-driven convective flows in these systems.

While we report a surface tension change at a position remote from the spreading drop, it must be recognized that the surface concentration outside the drop is not uniform during spreading.[27] A 1 μL drop of 2 mM SDS solution deposited on the PA solution subphase in a 7.5 cm radius dish at a distance of either 4 or 6 cm from the pin produced a maximum surface tension decrease of 1.1 ± 0.1 or 0.6 ± 0.1 mN/m, respectively (n = 8 in each case). These results also include an areal dilution of surfactant as it spreads.

After the surfactant drop deposition, the surface tension passes through a minimum and starts to recover (see Figure 5). The surface tension decrease is caused by the escaping surfactant, but the radial surface convection of surfactant is accompanied by dissolution into the subphase in the normal direction. Once the finite surfactant supply in the drop is depleted or the surfactant flux from the drop onto the surface slows compared to the dissolution rate of the escaped surfactant into the subphase, the surface tension recovers. This slower recovery of the subphase surface tension occurs over tens of seconds after passing through the minimum. This is characteristic of a soluble surfactant. In contrast, Figure 6 shows a rapid decrease but no recovery in surface tension after depositing a 1 μL drop of pure oleic acid, an insoluble surfactant, on a PA solution subphase.

Figure 7 shows a typical surface tension recovery profile after attaining minimum surface tension on deposition of a 1 μL drop of 2 mM SDS solution. The recovery of surface tension is exponential, as predicted by Lee and Starov for diffusion of a soluble surfactant into the subphase.[23,24] Because of the slow continual background drift in the PA solution surface tension, it

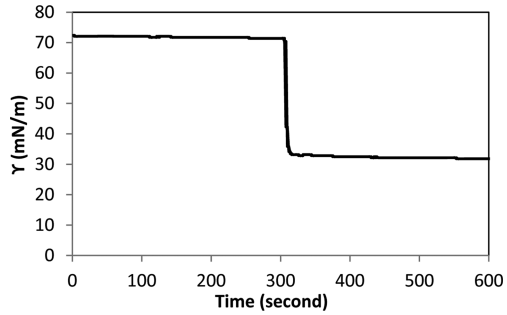

Figure 6. Surface tension of 1 wt %/wt PA subphase before and after deposition of a 1 μL drop of oleic acid at 4 cm from the pin at $t \sim 300$ s.

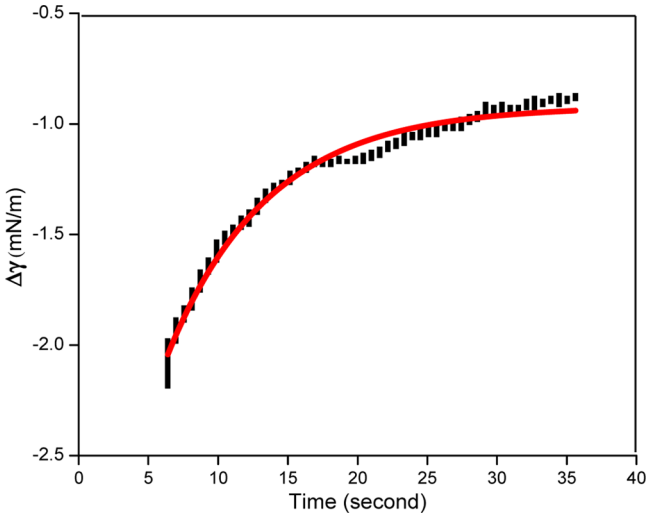

Figure 7. Typical plot showing exponential recovery of surface tension after depositing a 1 μL drop of 2 mM SDS solution on a 1 wt %/wt PA subphase. The red line shows an exponential fit.

was impossible to determine how much of the surfactant had diffused into the subphase during the time frame of the experiment.

The surfactant front moves faster than the drop contact line that is feeding surfactant to the monolayer as it convects radially outward. The surface tension decrease occurred at the Wilhelmy pin 4 cm away from the deposition point within 1 s of deposition. We visually observed that the spreading of the drop was still in progress at that time. This confirms a key prediction made by earlier models of spreading surfactant drops on liquid subphases.[19,44] Using different systems and experimental techniques, we have previously observed the surfactant front leading the contact line after depositing drops of an insoluble surfactant deposited on a simple glycerol–water subphase (75% v/v)[33] and for drops of SDS solutions deposited on a mucin solution subphase.[7]

It is informative to estimate how the surfactant inventory partitions between the drop and interface and how this relates to the final extent of the spread drop. The maximum surface tension decrease, i.e., the maximum surface pressure, contains information about the maximum surfactant surface excess concentration at the location of the Wilhelmy pin (~4 cm from the deposition point). Although the situation is highly dynamic, we estimate the maximum surface excess concentration assuming local equilibrium. Microscopic reversibility then allows us to apply a surface equation of state to extract the instantaneous surface excess concentration from the instantaneous surface pressure. The small surface pressure produced is consistent with a dilute monolayer, which suggests that Henry's law regime of the suface equation of state[45]

$$\Pi = RT\Gamma \tag{5}$$

is appropriate, where Π is the surface pressure, R is the universal gas constant, T is the temperature, and Γ is the surface excess concentration.

The surface excess concentration in the monolayer outside the spreading drop needed to produce a 1 mN/m surface pressure is 0.2 molecules/nm^2. To estimate the total number of surfactant molecules that resided in the monolayer at the point of maximum surface pressure, we assume they reside in an annulus bounded on the outside by a circle of radius 4 cm (the radial distance of the pin from the deposition point) and on the inside by a circle of radius 2 cm, the average final radius of the drop after convective spreading. Multiplying the surface excess concentration by the area of this annulus, we estimate that the number of escaped SDS molecules is on the order of 3×10^{14}. This represents 25% of the total number of SDS molecules contained in the 1 μL, 2 mM drop. This estimate is a lower bound, since surfactant molecules are also dissolving into the subphase. Moreover, all theoretical surfactant spreading models predict that the surfactant concentration on the surface decreases from the drop's contact line to the leading edge of the surfactant front.[27] Recall (from section 3.2) that the maximum surface pressure was less when the pin was moved further from the deposition point, consistent with these ideas.

Thus, the process of surfactant crossing the contact line and spreading across the subphase significantly depletes surfactant from the drop while spreading is in progress. As this depletion occurs, the drop/vapor surface tension must increase, and this increase alters the capillary balance that dictates the shape of the drop. Consistent with such an increase in drop/vapor surface tension, we observe a decrease in its spread diameter, or the retraction of the lens, on a time scale comparable to that of surfactant dissolution. The drop spreads to its maximum spread diameter within 2–3 s of deposition and then retracts over a period of about a minute. The recoil phenomenon due to surfactant depletion from the lens has been modeled by others.[44]

3.3. Fate of the Dye. Figure 3b shows the fluorescein dye image when the drop lens in Figure 3a is viewed in epi-illumination mode. Both parts a and b of Figure 3 are identical in shape, suggesting that the dye does not escape the lens. In Figure 3c, we superimpose a dye emission intensity line scan from Figure 3b with the Ronchi ruling image locating the edge of the lens. Clearly the hydrophilic fluorescein dye remains in the lens. In fact, we find that the dye stays in the lens throughout the spreading process. We detect no dye entrained in the advancing layer of surfactant with a detectability limit of of about one dye molecule per 10^4 Å^2 (see the Supporting Information). Since it is only the amphiphilic surfactant molecules that create the Marangoni stress, they are the only molecules that are driven to cross the drop contact line. There is no strong thermodynamic driving force to pull the hydrophilic dye out of the drop other than the attendent entropy increase.

4. CONCLUSIONS

The spreading of a soluble surfactant solution from a fully miscible drop deposited on an entangled polymer solution

dx.doi.org/10.1021/am400762q | ACS Appl. Mater. Interfaces 2013, 5, 5542–5549

proceeds by a cascade of events characterized by a number of transport processes involving different system components with a range of time scales. When the drop touches the surface, it immediately starts to spread because of the capillary imbalance established at the contact line. For the entangled polymer subphase and soluble surfactant system examined here, the spreading is complete in a few seconds. During the spreading, surfactant escapes the drop across the contact line and moves rapidly across the surface of the subphase at speeds on the order of cm/s. As predicted in prior literature, this spreading is driven by Marangoni stresses arising from the surfactant concentration gradients that develop immediately on drop deposition. The leading edge of the surfactant front moves faster than the contact line of the spreading drop. The surfactant layer at the interface is depleted by dissolution into the bulk subphase on time scales on the order of tens of seconds, approximately an order of magnitude larger than the spreading times of the drop or expanding surfactant layer. The expanding surfactant layer significantly depletes the drop of its surfactant. The amount of surfactant that can be depleted from the drop of course depends on the total surface area of the liquid subphase and the surfactant inventory in the drop.

Small areas and drops having larger surfactant inventories would reduce the extent of drop depletion during the spreading event, before dissolution into the bulk becomes significant. The surfactant depletion from the drop increases the drop/vapor surface tension and causes a retraction of the drop on the same time scale as the dissolution of the surfactant into the subphase. A non-surface-active hydrophilic solute mimicking drug does not partition with the escaping surfactant layer and remains with the drop without crossing the contact line.

Even though all the components of the drop are completely soluble in the subphase, a lens of solvent remains on the surface for several minutes after spreading is complete. This retention of solvent in the form of a lens arises because the fluid motions during spreading have not convectively intermixed the drop and subphase contents and the diffusive movement of polymer chains out of the subphase into the lens is exceedingly slow. This result also offers an explanation for the apparent independence of the qualitative spreading behavior from the chemical nature of the surfactant and of the subphase polymers observed in our prior work:[7] the quasi-immiscibility of the drop and subphase solutions during the spreading event suggests that the bulk surfactant and the bulk subphase polymer do not come into intimate contact during spreading; hence, the specific chemistries of the surfactant and polymer do not come into play during spreading. Thus, the selection of appropriate surfactants for lung delivery may be based more on physical criteria such as solubility and CMC as well as toxicity considerations rather than on the need for a specific chemistry.

Our results also suggest that an additional spreading mechanism could come into play when translating individual drop spreading behavior to that of many droplets deposited from an aerosol in the lung. It is plausible that the hydrodynamic disturbance and/or the surface pressures created by the escaped surfactant could repel the individual aerosol droplets away from each other after deposition on the subphase. This repulsion between individual droplets could expand the entire field of deposited droplets, thereby increasing the total spread area. In regions of the lungs where aerosol deposition fluxes are sufficiently low such that less than a monolayer of aerosol droplets is created, as expected downstream of a partial obstruction, for example, this repulsion may be the dominant mechanism of postdeposition drug transport. This may give rise to a new pulmonary delivery opportunity in the most problematic regions of diseased lung airways: spreading aerosolized surfactant-laden droplets after deposition using the mutual lateral hydrodynamic/surface pressure repulsions arising from their advancing surfactant monolayers. Macroscopic evidence of enhanced spreading of different aerosolized surfactant solutions[6] combined with considerations of the transport mechanism and fate of surfactant and hydrophilic solutes for individual deposited drops reported here will help guide the formulation of inhaled liquid aerosol drug delivery systems designed to maximize spreading in the lungs.

■ ASSOCIATED CONTENT

Ⓢ Supporting Information

Figures showing the dependence of the viscosity of PA solutions on PA concentration and representative plots showing surface tension change when a 1 μL drop of 1 mM SDS is deposited on the 1 wt %/wt PA solution subphase. Description of the estimation of the fluorescein detectability limit of the microscope. This material is available free of charge via the Internet at http://pubs.acs.org.

■ AUTHOR INFORMATION

Corresponding Author

*E-mail: sg2e@andrew.cmu.edu.

Notes

The authors declare no competing financial interest.

■ ACKNOWLEDGMENTS

This material is based on work supported in part by the National Science Foundation under grants CBET-0931057 and DMS-0635983 and in part by the National Heart, Lung and Blood Institute at the National Institutes of Health under grant number R01 HL105470. Its contents are solely the responsibility of the authors and do not necessarily represent the official views of NHLBI. R.S. would like to acknowledge the Thomas and Adrienne Klopack Graduate Fellowship.

■ REFERENCES

(1) Smaldone, G. C.; Palmer, L. B. *Respir. Care* **2002**, *45*, 667−675.
(2) Svartengren, K.; Lindestad, P. A.; Svartengren, M.; Bylin, G.; Philipson, K.; Camner, P. *Eur. Respir. J.* **1994**, *7*, 1467−1473.
(3) Corcoran, T. E. *Adv. Drug Delivery Rev.* **2006**, *58*, 1119−1127.
(4) Brown, J. S.; Zeman, K. L.; Bennett, W. D. *J. Aerosol Med.* **2001**, *14*, 443−454.
(5) Corocoran, T. E.; Thomas, K. M.; Garoff, S.; Tilton, R. D.; Przybycien, T. M.; Pilewski, J. M. *J. Aerosol Med. Pulm. Drug Delivery* **2012**, *25*, 290−296.
(6) Marcinkowski, A. L.; Garoff, S.; Tilton, R. D.; Pilewski, J. M.; Corcoran, T. E. *J. Aerosol Med. Pulm. Drug Delivery* **2008**, *21*, 361−369.
(7) Koch, K.; Dew, B.; Corcoran, T. E.; Przybycien, T. M.; Tilton, R. D.; Garoff, S. *Mol. Pharm.* **2011**, *8*, 387−394.
(8) Grotberg, J. B. *Annu. Rev. Biomed. Eng.* **2001**, *3*, 421−457.
(9) Grotberg, J. B.; Gaver, D. P. *J. Colloid Interface Sci.* **1996**, *178*, 377−378.
(10) Halpern, D.; Jensen, O. E.; Grotberg, J. B. *J. Appl. Physiol.* **1998**, *85*, 333−352.
(11) Matar, O. K.; Craster, R. V.; Warner, M. R. E. *J. Fluid Mech.* **2002**, *466*, 85−111.
(12) Zhang, Y. L.; Matar, O. K.; Craster, R. V. *J. Non-Newtonian Fluid Mech.* **2002**, *105*, 53−78.
(13) Jensen, O. E.; Grotberg, J. B. *J. Fluid Mech.* **1992**, *240*, 259−288.

(14) Craster, R. V.; Matar, O. K. *J. Fluid Mech.* **2000**, *425*, 235−258.
(15) Kaneko, D.; Gong, J. P.; Zrinyl, M.; Osada, Y. *J. Polym. Sci., Part B: Polym. Phys.* **2005**, *43*, 562−572.
(16) Fallest, D. W.; Lichtenberger, A. M.; Fox, C. F.; Daniels, K. E. *New J. Phys.* **2010**, *12*, No. 073029.
(17) Gaver, D. P.; Grotberg, J. B. *J. Fluid Mech.* **1992**, *235*, 399−414.
(18) Starov, V. M.; deRyck, A.; Velarde, M. G. *J. Colloid Interface Sci.* **1997**, *190*, 104−113.
(19) Dussaud, A. D.; Matar, O. K.; Troian, S. M. *J. Fluid Mech.* **2005**, *544*, 23−51.
(20) Afsar-Siddiqui, A. B.; Luckham, P. F.; Matar, O. K. *Langmuir* **2004**, *20*, 7575−7582.
(21) Afsar-Siddiqui, A. B.; Luckham, P. F.; Matar, O. K. *Langmuir* **2003**, *19*, 703−708.
(22) Afsar-Siddiqui, A. B.; Luckham, P. F.; Matar, O. K. *Langmuir* **2003**, *19*, 696−702.
(23) Lee, K. S.; Starov, V. M. *J. Collloid Interface Sci.* **2009**, *329*, 361−365.
(24) Lee, K. S.; Starov, V. M. *J. Collloid Interface Sci.* **2007**, *314*, 631−642.
(25) Hanyak, M.; Sinz, D.; Darhuber, A. *Soft Matter* **2012**, *8*, 7660−7671.
(26) Afsar-Siddiqui, A. B.; Luckham, P. F.; Matar, O. K. *Adv. Colloid Interface Sci.* **2003**, *106*, 183−236.
(27) Matar, O. K.; Craster, R. V. *Soft Matter* **2009**, *5*, 3801−3809.
(28) Craster, R. V.; Matar, O. K. *Rev. Mod. Phys.* **2009**, *81*, 1131−1198.
(29) Berg, S. *Phys. Fluids* **2009**, *21*, No. 032105.
(30) Samet, J. M.; Cheng, P. W. *Environ. Health Perspect.* **1994**, *102*, 89−103.
(31) Verdugo, P.; Tam, P. Y.; Butler, J. *Biorheology* **1983**, *30*, 223−230.
(32) Bansil, R.; Stanley, E.; LaMont, J. T. *Annu. Rev. Physiol.* **1995**, *57*, 635−657.
(33) Sharma, R.; Kalita, R.; Swanson, E. R.; Corcoran, T. E.; Garoff, S.; Przybycien, T. M.; Tilton, R. D. *Langmuir* **2012**, *28*, 15212−15221.
(34) Hu, R. Y. Z. *Exp. Therm. Fluid Sci.* **1991**, *4*, 723−729.
(35) Hai, M.; Han, B.; Yan, H.; Han, Q. *J. Chem. Eng. Data* **1998**, *43*, 1056−1058.
(36) Noskov, B. A.; Akentiev, A. V.; Bilibin, A. Y.; Zorin, I. M.; Miller, R. *Adv. Colloid Interface Sci.* **2003**, *104*, 245−271.
(37) Pauchard, L.; Allain, C. *Europhys. Lett.* **2003**, *62*, 897−903.
(38) David, A. E. *Chem. Eng. Commun.* **1998**, *166*, 201−216.
(39) Okuzono, T.; Ozawa, K.; Doi, M. *Phys. Rev. Lett.* **2006**, *97*, No. 136103.
(40) Banaha, M.; Daerr, A.; Limat, L. *Eur. Phys. J.: Spec. Top.* **2009**, *166*, 185−188.
(41) Kim, J. H.; Domach, M. M.; Tilton, R. D. *Langmuir* **2000**, *16*, 10037−10043.
(42) Spandagos, C.; Goudoulas, T. B.; Luckham, P. F.; Matar, O. K. *Langmuir* **2012**, *28*, 7197−7211.
(43) Evans, D. F.; Mukherjee, S.; Mitchell, D. J.; Ninham, B. W. *J. Colloid Interface Sci.* **1983**, *93*, 184−204.
(44) Karapetsas, G.; Craster, R. V.; Matar, O. K. *Phys. Fluids* **2011**, *23*, No. 122106.
(45) Berg, J. C. *An Introduction to Interfaces & Colloids: The Bridge to Nanoscience*; World Scientific Publishing: Singapore, 2010; p 134.